Progress of Theoretical Physics, Vol. 70, No. 5, November 1983

Stability Theory of Synchronized Motion in Coupled-Oscillator Systems. II

—— *The Mapping Approach* ——

Tomoji YAMADA and Hirokazu FUJISAKA*

Department of Physics, Kyushu Institute of Technology
Kitakyushu 804
**Department of Physics, Kagoshima University, Kagoshima 890*

(Recevied August 8, 1983)

The coupled-oscillator system described by differential equations is studied by a mapping. The mapping function for the coupled system is derived from the one for the uncoupled system. The bifurcation diagram is examined first by numerically integrating the coupled differential equations and second by iterating the mapping for the coupled system. Both approaches give quite similar results: Especially the transition from the uniform chaos to the non-uniform one occurs at the same value of the bifurcation parameter for both approaches.

§ 1. Introduction

In a previous paper of this series (referred to as I) the global stability of a macrooscillation is considered.[1] The consideration is made on the system consisting of N-equivalent oscillators. The state vector of the j-th oscillator $\boldsymbol{x}^{(j)}$ evolves in time as

$$\dot{\boldsymbol{x}}^{(j)}=\boldsymbol{f}(\boldsymbol{x}^{(j)};\, t)+D\sum_{l}{}_{\text{conf}}(\boldsymbol{x}^{(l)}-\boldsymbol{x}^{(j)}),\qquad j=1,2,\cdots,N, \tag{1·1}$$

where the summation is taken over a given configuration of coupling and $\boldsymbol{f}$ is a periodic function of the period $2\pi/\omega$ with respect to the variable t. When the scalar coupling strength D exceeds a certain value, the macrooscillation or the synchronized state Ψ_{unif} appears. Below this critical D value the synchronized state loses the stability and a non-uniform state arises. Further variation of D brings about various states and a bifurcation scheme.

In various systems described by differential equations an appropriate discretization in time leads to the appearance of mapping functions.[2] This discretization can be done by taking a Lorenz plot or a Poincaré map Therefore in these systems the time evolutions of dynamical variables at discrete time can be obtained by simply iterating the mappings.

In the present paper we will consider the coupled system (1·1) in the case where the uncoupled system,

$$\dot{\boldsymbol{x}}^{(j)}=\boldsymbol{f}(\boldsymbol{x}^{(j)};\, t), \tag{1·2}$$

has the mapping,

$$\boldsymbol{x}_{n+1}^{(j)}=\boldsymbol{g}(\boldsymbol{x}_{n}^{(j)}), \tag{1·3}$$

where $\boldsymbol{x}_n{}^{(j)}$ is the state vector of the j-th oscillator at time, $t=nT$ $(n=0,1,2,\cdots)$. When the coupling terms are introduced, the description by the mapping should be modified. The purpose of the present paper is to show that even for the coupled system a mapping

approach is possible with an appropriate modification of the mapping function. Thus the temporal behaviors of coupled system can be obtained by simple iterations of the resulting modified mapping.

A coupled mapping system has been studied by Kaneko,[3] and Lee and Tomita.[4] Their equations can be written as follows:

$$\begin{aligned} x_{n+1}^{(1)} &= g(x_n^{(1)}) + D(x_n^{(2)} - x_n^{(1)}), \\ x_{n+1}^{(2)} &= g(x_n^{(2)}) + D(x_n^{(1)} - x_n^{(2)}), \end{aligned} \tag{1·4}$$

where g is a one-dimensional mapping and D is a coupling constant. From these equations various states including a hyperchaos are obtained. However, for a large D value, $|x_n{}^{(2)} - x_n{}^{(1)}| \to \infty$ as $n \to \infty$.[4] Therefore, Eqs. (1·4) cannot be correct basic mapping equations corresponding to system (1·1).

In § 2 we will derive a mapping which correctly gives the large coupling limit of the coupled system. In § 3 this mapping will be examined for simple illustrative examples. In § 4 the mapping will be applied to a particular model and the results will be compared with those calculated from the original coupled differential equations. Section 5 will be devoted to summary and discussion.

§ 2. The mapping for the coupled system

Now we consider the N-equivalent oscillator system (1·1). By introducing a new state vector,

$$\boldsymbol{X} = \begin{pmatrix} \boldsymbol{x}^{(1)} \\ \boldsymbol{x}^{(2)} \\ \vdots \\ \boldsymbol{x}^{(N)} \end{pmatrix}, \tag{2·1}$$

Eq. (1·1) can be written in the form

$$\frac{d\boldsymbol{X}}{dt} = \boldsymbol{F}(\boldsymbol{X};t) + \bar{D}\boldsymbol{X}, \tag{2·2}$$

where $\boldsymbol{F}$ is the flow defined by

$$\boldsymbol{F} = \begin{pmatrix} \boldsymbol{f}(\boldsymbol{x}^{(1)};t) \\ \boldsymbol{f}(\boldsymbol{x}^{(2)};t) \\ \vdots \\ \boldsymbol{f}(\boldsymbol{x}^{(N)};t) \end{pmatrix} \tag{2·3}$$

and $\bar{D}$ is the diffusion matrix whose explicit form depends on the given configuration of coupling. For simplicity, we will hereafter consider the special case, System I of I, where all oscillators couple:[1] namely,

$$\sum_{l}{}_{\text{conf}}(\boldsymbol{x}^{(l)} - \boldsymbol{x}^{(j)}) = \sum_{l=1}^{N}(\boldsymbol{x}^{(l)} - \boldsymbol{x}^{(j)}). \tag{2·4}$$

It is to be noted that for $N = 2$ and 3 System I is equivalent to System II.[1] For the present configuration of coupling $\bar{D}$ is written as

$$\bar{D}\equiv D\hat{C}=D\begin{pmatrix} -(N-1)\hat{1}_m & \hat{1}_m & \cdots & \hat{1}_m \\ \hat{1}_m & -(N-1)\hat{1}_m & & \hat{1}_m \\ \vdots & & \ddots & \\ \hat{1}_m & \cdots & & -(N-1)\hat{1}_m \end{pmatrix}, \tag{2·5}$$

where $\hat{1}_m$ denotes the $m\times m$ unit matrix and m is the number of components of the state vectors $\{\boldsymbol{x}^{(j)}\}$.

Defining the vector $\boldsymbol{Y}$ as

$$\boldsymbol{Y}=\exp\{-\bar{D}(t-t_n)\}\boldsymbol{X}, \tag{2·6}$$

we have

$$\frac{d\boldsymbol{Y}}{dt}=\exp\{-\bar{D}(t-t_n)\}\boldsymbol{F}(\exp\{\bar{D}(t-t_n)\}\boldsymbol{Y};t), \tag{2·7}$$

where $t_n=nT(n=0,1,2,\cdots)$ with a constant T. From the calculation given in Appendix A, we obtain

$$\exp(\bar{D}t)=\hat{1}+\xi_D^{(N)}(t)\hat{C}, \tag{2·8}$$

where

$$\xi_D^{(N)}(t)=\{1-\exp(-NDt)\}/N. \tag{2·9}$$

Here $\hat{1}$ is the unit matrix and the matrix $\hat{C}$ defined in (2·5) is used. By writing the vector $\boldsymbol{Y}$ as

$$\boldsymbol{Y}=\begin{pmatrix} \boldsymbol{y}^{(1)} \\ \boldsymbol{y}^{(2)} \\ \vdots \\ \boldsymbol{y}^{(N)} \end{pmatrix}, \tag{2·10}$$

a simple calculation yields

$$\boldsymbol{x}^{(i)}=\boldsymbol{y}^{(i)}+\xi_D^{(N)}(t-t_n)\sum_{j=1}^{N}(\boldsymbol{y}^{(j)}-\boldsymbol{y}^{(i)}), \qquad i=1,2,\cdots,N. \tag{2·11}$$

In terms of $\{\boldsymbol{y}^{(i)}\}$, Eq. (2·7) can be written as

$$\dot{\boldsymbol{y}}^{(i)}=\boldsymbol{f}(\boldsymbol{x}^{(i)};t)+\xi_{-D}^{(N)}(t-t_n)\sum_{j=1}^{N}\{\boldsymbol{f}(\boldsymbol{x}^{(j)};t)-\boldsymbol{f}(\boldsymbol{x}^{(i)};t)\}. \tag{2·12}$$

As is proved in Appendix B, Eq. (2·12) can be approximated,

$$\dot{\boldsymbol{y}}^{(i)}\simeq\boldsymbol{f}(\boldsymbol{y}^{(i)};t), \tag{2·13}$$

if the second order deviations of the state vectors from the macrooscillation are discarded. Equation (2·13) is just the same as (1·2). Therefore, if the uncoupled system has the mapping (1·3), we obtain for $i=1,2,\cdots,N$

$$\boldsymbol{y}_{n+1}^{(i)}=\boldsymbol{g}(\boldsymbol{y}_n^{(i)}), \tag{2·14}$$

where $\boldsymbol{y}_{n+1}^{(i)}$ and $\boldsymbol{y}_n^{(i)}$ are the vectors $\boldsymbol{y}^{(i)}$ at time $t=t_{n+1}=(n+1)T$ and $t_n=nT$, respectively. Since $\xi_D^{(N)}(0)=0$, $\boldsymbol{x}_n^{(i)}=\boldsymbol{y}_n^{(i)}$ at $t=t_n$. By putting $t=t_{n+1}$ in (2·11), we have

$$\boldsymbol{x}_{n+1}^{(i)}=\boldsymbol{y}_{n+1}^{(i)}+\xi_D^{(N)}(T)\sum_{j=1}^{N}(\boldsymbol{y}_{n+1}^{(j)}-\boldsymbol{y}_{n+1}^{(i)}). \tag{2·15}$$

Use of (2·14) and (2·15) yields

$$\boldsymbol{x}_{n+1}^{(i)}=\boldsymbol{g}(\boldsymbol{x}_n^{(i)})+\xi_D^{(N)}(T)\sum_{j=1}^{N}\{\boldsymbol{g}(\boldsymbol{x}_n^{(j)})-\boldsymbol{g}(\boldsymbol{x}_n^{(i)})\}. \tag{2·16}$$

Hereafter we will use the terminologies, the mapping approach and the differential equation approach when use are made of Eqs. (2·16) and (1·1) as the basic equations, respectively.

§ 3. Simple examples

When the number of oscillators N is equal to 2 and the mapping $\boldsymbol{g}$ is reduced to a one-dimensional map, Eq. (2·16) becomes

$$\begin{aligned}x_{n+1}^{(1)}&=g(x_n^{(1)})+\xi_D^{(2)}(T)\{g(x_n^{(2)})-g(x_n^{(1)})\},\\ x_{n+1}^{(2)}&=g(x_n^{(2)})+\xi_D^{(2)}(T)\{g(x_n^{(1)})-g(x_n^{(2)})\},\end{aligned} \tag{3·1}$$

where $x_n^{(i)}(i=1,2)$ is a component of the state vector $\boldsymbol{x}_n^{(i)}$ and g is the corresponding one-dimensional mapping. This equation can be written in the following form:

$$\begin{aligned}x_{n+1}^{(1)}&=g(x_n^{(1)})+D'(x_{n+1}^{(2)}-x_{n+1}^{(1)}),\\ x_{n+1}^{(2)}&=g(x_n^{(2)})+D'(x_{n+1}^{(1)}-x_{n+1}^{(2)})\end{aligned} \tag{3·2}$$

with $D'=\{\exp(2DT)-1\}/2$. This has the same form as Eq. (1·4), but in the coupling terms $x_n^{(i)}$are replaced by $x_{n+1}^{(i)}(i=1,2)$.

In a large D limit, $\xi_{D=\infty}^{(2)}=1/2$ and then $x_{n+1}^{(1)}=x_{n+1}^{(2)}$. This means that for a large coupling strength the synchronized state Ψ_{unif} appears.[1] The synchronized state or the macrooscillation loses stability as D is decreased. The stability problem of the macrooscillation can be treated by the analogous method developed in I.[1] Let x_{0n} be a solution of (3·1) in Ψ_{unif}. The $x_n^{(i)}$ can be written as $x_n^{(i)}=x_{0n}+u_n^{(i)}$, where $u_n^{(i)}$ is the deviation from Ψ_{unif}. Up to the first order in $u_n^{(i)}$ we get,

$$r_{n+1}=(1-2\xi_D^{(2)}(T))g'(x_{0n})r_n, \tag{3·3}$$

where $r_n\equiv u_n^{(2)}-u_n^{(1)}$ and g' is the derivative of g. Therefore the stability of Ψ_{unif} is determined by the sign of the following quantity:

$$\lambda'=\langle\log|\{1-2\xi_D^{(2)}(T)\}g'(x_{0n})|\rangle/T, \tag{3·4}$$

where$\langle\cdots\rangle$ denotes the time average. Simple calculation gives

$$\lambda'=\lambda_L-2D, \tag{3·5}$$

where λ_L is the largest Lyapunov exponent in Ψ_{unif}.*) For chaotic Ψ_{unif}, $\lambda_L>0$ and the macrooscillation become unstable at $D=D_c=\lambda_L/2$. The threshold value D_c is exactly the same as the one derived in the differential equation system (1·1). The results obtained in this section can be easily extended for general mappings and arbitrary N.

*) In the present paper the Lyapunov exponents for the mapping are defined by dividing the usual definition by T.[5] Thus Lyapunov exponents for the mapping and the differential equation coincide with each other.

§ 4. Coupled Brusselator model

In this section a concrete model is studied with the mapping approach developed in § 2 and the differential equation approach. We consider the model studied by Tomita and Kai.[5] The flow $\boldsymbol{f}$ and the state vector $\boldsymbol{x}$ of the model are given by

$$\boldsymbol{f}=\begin{pmatrix} x^2y-Bx+A-x \\ Bx-x^2y \end{pmatrix}+\begin{pmatrix} \tilde{a} \\ 0 \end{pmatrix}, \qquad \boldsymbol{x}=\begin{pmatrix} x \\ y \end{pmatrix} \tag{4·1}$$

with $\tilde{a}=a\cos(\omega t)$. Without the external force $\tilde{a}$, this is nothing but the Brusselator model.[6] Hereafter the following set of parameters is adopted: $A=0.4$, $B=1.2$, $a=0.05$ and $\omega=0.8$. For these parameter values the uncoupled system described by

$$\dot{\boldsymbol{x}}=\boldsymbol{f} \tag{4·2}$$

shows a chaotic behavior. The largest Lyapunov exponent of the chaos is numerically calculated as $\lambda_L\simeq 0.01398$. We here denote the value of x at time $t=t_n=(8\pi/\omega)n$ as $x_n(n=0,1,2,\cdots)$. Then the succesive x_n's form the one-dimensional map, $x_{n+1}=g(x_n)$, which is shown in Fig. 1. The mapping function g is approximated by a power series whose coefficients are given in Table I.

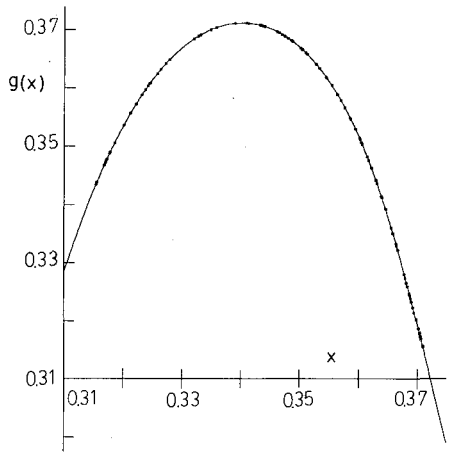

Fig. 1. The mapping function g for the coupled model considered in the present text. The full line is calculated from the power series in Table I and the dots are obtained by numerically integrating the uncoupled system (4·2).

The two oscillator system is constructed by introducing coupling between two oscillators whose state vectors are

$$\boldsymbol{x}^{(1)}=\begin{pmatrix} x^{(1)} \\ y^{(1)} \end{pmatrix}, \qquad \boldsymbol{x}^{(2)}=\begin{pmatrix} x^{(2)} \\ y^{(2)} \end{pmatrix}, \tag{4·3}$$

respectively. The time evolution of the coupled system is described by

$$\begin{aligned} \dot{\boldsymbol{x}}^{(1)}&=\boldsymbol{f}(\boldsymbol{x}^{(1)};t)+D(\boldsymbol{x}^{(2)}-\boldsymbol{x}^{(1)}), \\ \dot{\boldsymbol{x}}^{(2)}&=\boldsymbol{f}(\boldsymbol{x}^{(2)};t)+D(\boldsymbol{x}^{(1)}-\boldsymbol{x}^{(2)}), \end{aligned} \tag{4·4}$$

where the flow $\boldsymbol{f}$ is given by (4·1). Equation (4·4) is numerically simulated by using the Runge-Kutta-Gill method with the time step $(2\pi/\omega)/50$. The bifurcation diagram is examined by starting with, $\boldsymbol{x}^{(1)}=(0.35,2.75)$ and $\boldsymbol{x}^{(2)}=(0.32,2.50)$ at $D=0$, and increasing

Table I. The expansion coefficients of the mapping function $g(x)\equiv x_0+\sum_{l=0}^{10}C_l(x-x_0)^l$.

x_0	0.34943956	C_5	-0.19918181×10^{6}
C_0	0.18080436×10^{-1}	C_6	0.31899196×10^{7}
C_1	-0.81428963	C_7	0.48947795×10^{9}
C_2	-0.51875687×10^{2}	C_8	0.18738313×10^{11}
C_3	-0.74237535×10^{3}	C_9	0.32766486×10^{12}
C_4	-0.20892060×10^{5}	C_{10}	0.24180756×10^{13}

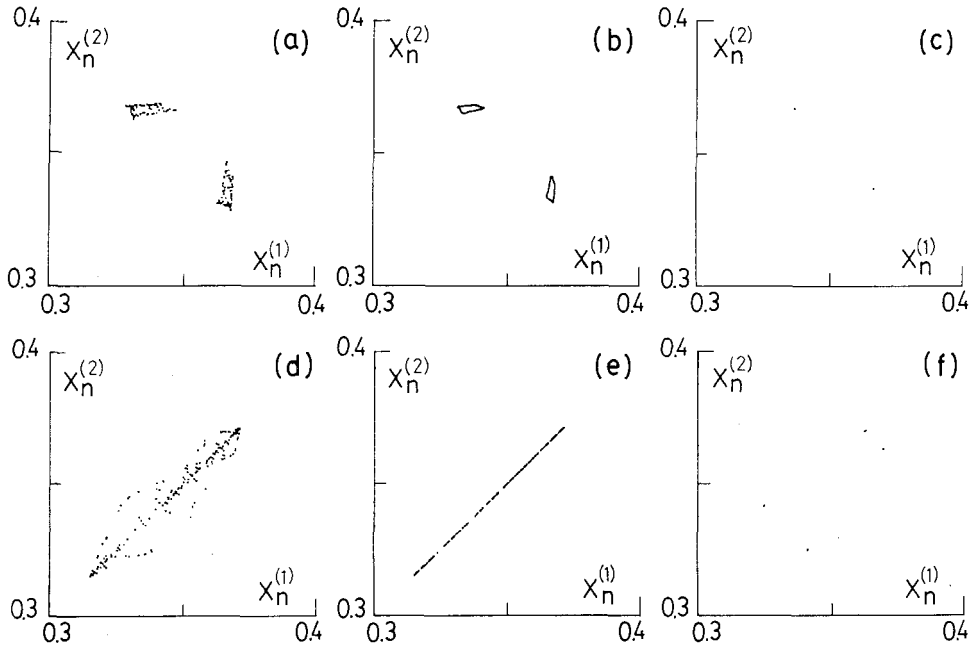

Fig. 2. The Poincaré maps: (a) $D=0.0026$, chaos C_I, (b) $D=0.0031$, quasiperiodic state Q. P, (c) $D=0.0040$, periodic state P, (d) $D=0.0066$,chaos C_{II}, (e) $D=0.0075$, chaos C_{III}, (f) $D=0.0059$, periodic state.

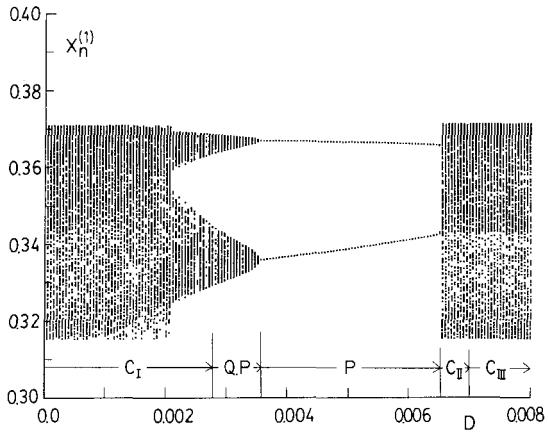

Fig. 3. The bifurcation scheme by the differential equation approach with the iterated value of $x_n^{(1)}$.

the coupling strength D by 0.00005 until 0.008. The state vectors of the preceding calculation are set to be the initial condition for the increased coupling strength. The phase of the system is determined by taking the Poincaré map and calculating the Lyapunov exponent after sufficiently large initial time steps. The Poincaré map is obtained by taking the projection of the state vectors on $(x^{(1)}, x^{(2)})$ plane at $t=t_n$. The values of $x^{(1)}$ and $x^{(2)}$ at $t=t_n$ are denoted by $x_n^{(1)}$ and $x_n^{(2)}$, respectively. In Fig.2 the Poincaré maps for several D values are plotted. In Figs. 2(a)~(e) there appear five phases which we denote by C_I, Q.P, P, C_{II} and C_{III}, respectively. The C_I, C_{II} and C_{III} are chaotic states, Q.P is a quasiperiodic state and P is a periodic state which in the original unit corresponds to eight-periodic state. In the bifurcation diagram the periodic state shown in Fig.2(f) does not appear since this phase originates from other basins than considered here. The bifurcation diagram is illustrated in Fig.3 with the iterated values of $x_n^{(1)}$. The transition from the periodic state P to the chaos C_{II} is of the first order type. By using Eq. (3·25) of I the breakdown of the uniform chaos C_{III} occurs at $D=\lambda_L/2\simeq 0.00699$.*) This agrees with the present numerical calculation. In the bifurcation the window structures arise

*) It is to be noted that the coupling $\hat{D}/2$ in Eq. (1·3) in I should be read D in the present work (see (1·1)).

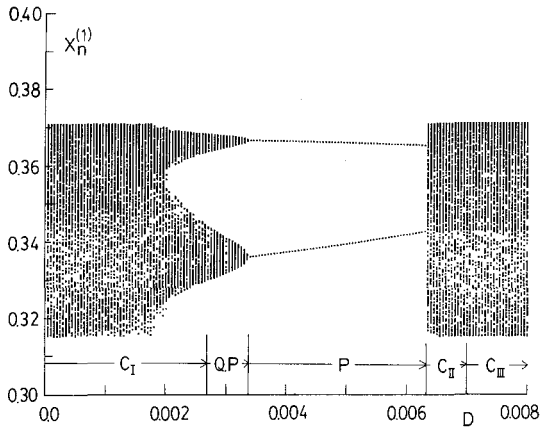

Fig. 4. The bifurcation scheme by the mapping approach with the iterated value of $x_n^{(1)}$.

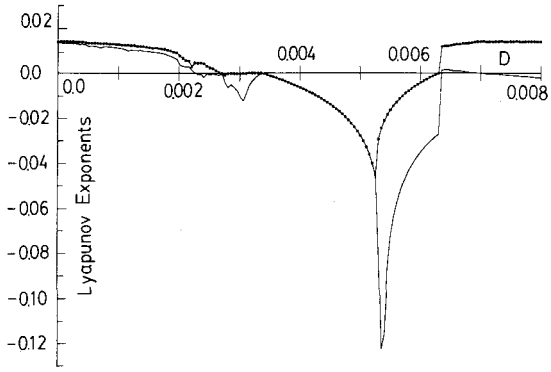

Fig. 5. The largest and the second largest Lyapunov exponents which are represented by the full line with black circles and the full line, respectively. These values are obtained by averaging over 70000 iterations. The jump of the Lyapunov exponents near $D=0.0063$ corresponds to the first order transition mentioned in § 4.

but they are omitted for simplicity.

Next we consider the bifurcation diagram of the coupled system with the mapping approach. The basic equations for $N=2$ are Eq. (3·1) with $T=8\pi/\omega$, where the mapping function g can be computed from Table I. A sequence of transitions is obtained by a similar procedure to the differential equation approach which is based on (4·4). The initial values are $x_{n=0}^{(1)}=0.35$ and $x_{n=0}^{(2)}=0.32$ for $D=0$ and the rest of procedure is the same as done for the differential equation approach. In Fig. 4 the bifurcation diagram with the iterated values of $x_n^{(1)}$ is shown. The sequence of transitions completely coincides with that of the differential equation approach though the values of transition points are slightly different. Quite similar Poincaré maps are obtained for the same values as in Fig. 2. The transition from P to C_{II} is also of the first order type. The largest and the second largest Lyapunov exponents are calculated by a similar method developed by Shimada and Nagashima[7] and plotted in Fig. 5. As seen from this figure the second largest Lyapunov exponent changes its sign at the transition point between C_{II} and C_{III}. The sign change of the second largest Lyapunov exponent also occurs at a small D. However, we cannot find any remarkable phase change at this D value.

§ 5. Summary and discussion

We have studied a coupled system by two approaches: the differential equation approach and the mapping approach. The basic equations of the latter approach are derived from the original coupled differential equations on the assumption that the deviations of the state vectors from those of the macrooscillation are small. Thus, the same value is obtained for the transition point from C_{II} to C_{III} by both approaches. For $D=0$ the system displays the same temporal behaviors of the state vectors for the two approaches as it should be. These facts explain why even for intermediate coupling strength there appear similar bifurcation schemes in both approaches.

We have been interested in the global bifurcation scheme. A transfer function can be defined through $x_{n+1}^{(1)}=h(x_n^{(1)})$, and numerically constructed in a chaos. In the present

case, however, the transfer function h does not lie on a single curve but rather forms a scattered band except the uniform chaos. Therefore, the bifurcation schemes studied in § 4 cannot be described by a one dimensional map. However it may be possible that the terminologies of one-dimensional map with external noise[8] can be applied to interpret the present results; for instance, the lack of the period doubling transition.

A continuous system can be also studied by the mapping approach. In this case the coupling is caused through diffusion and an appropriate extension of the mapping approach should be done, correspondingly. A chemical turbulence[9] is an example of the continuous system, where the spatial randomness is important as well as the temporal one. It is also interesting to extend our formulation to the case where the coupling D is not a scalar. These are future subjects.

Appendix A

The eigenvalue equation,

$$\det|\bar{D}-\lambda|=0, \tag{A·1}$$

has eigenvalues $\lambda=0$, $\lambda=-N$ which are m-and $m(N-1)$-fold degenerate, respctively. The matrix $\bar{D}$ is diagonalized as follows:

$$\hat{U}^{-1}\bar{D}\hat{U}=D\begin{pmatrix}\hat{0} & & \\ & -N\hat{1}_m & \\ & & \ddots \\ & 0 & & -N\hat{1}_m\end{pmatrix} \tag{A·2}$$

with

$$\hat{U}=\begin{pmatrix}\hat{1}_m & \hat{1}_m & \cdots & \hat{1}_m \\ \hat{1}_m-(N-1)\hat{1}_m & & & \hat{1}_m \\ \vdots & & \ddots & \\ \hat{1}_m & \cdots & & -(N-1)\hat{1}_m\end{pmatrix}. \tag{A·3}$$

From (A·2) one can easily get

$$\begin{aligned}\exp(\bar{D}t)&=\hat{1}-\hat{U}\begin{pmatrix}\hat{0} & & \\ & \hat{1}_m & \\ & & \ddots \\ & 0 & & \hat{1}_m\end{pmatrix}\hat{U}^{-1}(1-\exp(-NDt)) \\ &=\hat{1}+\xi_D^{(N)}\hat{C}.\end{aligned} \tag{A·4}$$

Appendix B

In the synchronized state Ψ_{unif} one has

$$\boldsymbol{x}^{(i)}=\boldsymbol{y}^{(i)}, \qquad i=1, 2, \cdots, N. \tag{B·1}$$

Therefore, if the state vectors do not deviate appreciably from those of the macrooscillation, the second term of (2·11) is small compared with the first term. Thus we expand

$\boldsymbol{f}(\boldsymbol{x}^{(i)})(\equiv\boldsymbol{f}(\boldsymbol{x}^{(i)};t))$ as

$$\boldsymbol{f}(\boldsymbol{x}^{(i)})=\boldsymbol{f}(\boldsymbol{y}^{(i)})+\xi_D{}^{(N)}\frac{\partial\boldsymbol{f}(\boldsymbol{y}^{(i)})}{\partial\boldsymbol{y}^{(i)}}\cdot\sum_{j=1}^{N}(\boldsymbol{y}^{(j)}-\boldsymbol{y}^{(i)})+O(|\delta\boldsymbol{y}|^2), \tag{B·2}$$

where

$$|\delta\boldsymbol{y}|\simeq|\boldsymbol{y}^{(i)}-(\sum_{j=1}^{N}\boldsymbol{y}^{(j)})/N|, \qquad (i=1,2,\cdots,N)$$

and represents the deviation of the state vector from the macrooscillation since it takes zero value in the synchronized state. Because of small $|\delta\boldsymbol{y}|$, we also obtain

$$\boldsymbol{f}(\boldsymbol{y}^{(j)})=\boldsymbol{f}(\boldsymbol{y}^{(i)})+\frac{\partial\boldsymbol{f}(\boldsymbol{y}^{(i)})}{\partial\boldsymbol{y}^{(i)}}\cdot(\boldsymbol{y}^{(j)}-\boldsymbol{y}^{(i)})+O(|\delta\boldsymbol{y}|^2). \tag{B·3}$$

Substitution of (B·2) and (B·3) into the right-hand side of (2·12) yields

$$\begin{aligned}\dot{\boldsymbol{y}}^{(i)}&=\boldsymbol{f}(\boldsymbol{y}^{(i)})+\xi_D{}^{(N)}\frac{\partial\boldsymbol{f}(\boldsymbol{y}^{(i)})}{\partial\boldsymbol{y}^{(i)}}\cdot\sum_{j=1}^{N}(\boldsymbol{y}^{(j)}-\boldsymbol{y}^{(i)})+\xi_{-D}{}^{(N)}\sum_{j=1}^{N}\{\boldsymbol{f}(\boldsymbol{y}^{(j)})-\boldsymbol{f}(\boldsymbol{y}^{(i)})\}\\&\quad+\xi_{-D}{}^{(N)}\xi_D{}^{(N)}\sum_{j=1}^{N}\sum_{l=1}^{N}\left\{\frac{\partial\boldsymbol{f}(\boldsymbol{y}^{(j)})}{\partial\boldsymbol{y}^{(j)}}\cdot(\boldsymbol{y}^{(l)}-\boldsymbol{y}^{(j)})-\frac{\partial\boldsymbol{f}(\boldsymbol{y}^{(i)})}{\partial\boldsymbol{y}^{(i)}}\cdot(\boldsymbol{y}^{(l)}-\boldsymbol{y}^{(i)})\right\}+O(|\delta\boldsymbol{y}|^2)\\&=\boldsymbol{f}(\boldsymbol{y}^{(i)})+O(|\delta\boldsymbol{y}|^2),\end{aligned} \tag{B·4}$$

where use has been made of the identity,

$$\xi_D{}^{(N)}+\xi_{-D}{}^{(N)}-N\xi_{-D}{}^{(N)}\xi_D{}^{(N)}=0.$$

References

1) H. Fujisaka and T. Yamada, Prog. Theor. Phys. **69** (1983), 32.
2) E. N. Lorenz, J. Atomos. Sci. **20** (1963), 130.
K. Tomita, Phys. Rep. **86** (1982), 113.
H. L. Swinney, Physica D, to appear.
J. P. Gollub, E. J. Romer and J. E. Socolar, J. Stat. Phys. **23** (1980), 321.
T. Yamada and R. Graham, Phys. Rev. Lett. **45** (1980), 1322.
3) K. Kaneko, Prog. Theor. Phys. **69** (1983), 1427.
4) Y. S. Lee and K. Tomita, to be published.
5) K. Tomita and T. Kai, Prog. Theor. Phys. Suppl. No. 61 (1978), 280.
6) I. Prigogine and R. Lefever, J. Chem. Phys. **48** (1968), 1965.
7) I. Shimada and T. Nagashima, Prog. Theor. Phys. **61** (1979), 1605.
8) J. P. Crutchfield and B. A. Huberman, Phys. Lett. **77A** (1980), 407.
9) Y. Kuramoto and T. Yamada, Prog. Theor. Phys. **56** (1976), 679.